Ab initio study of the critical thickness for ferroelectricity in ultrathin Pt/$PbTiO_3$/Pt films

Yoshitaka Umeno[1,2], Bernd Meyer[3], Christian Elsässer[4,1], and Peter Gumbsch[1,4]

[1] *IZBS, University of Karlsruhe, Kaiserstr. 12, 76131 Karlsruhe, Germany*

[2] *Graduate School of Engineering, Kyoto University, Sakyo-ku, Kyoto 606-8501, Japan*

[3] *Lehrstuhl für Theoretische Chemie, Ruhr-Universität Bochum, 44780 Bochum, Germany and*

[4] *Fraunhofer Institute for Mechanics of Materials IWM, Wöhlerstr. 11, 79108 Freiburg, Germany*

(Dated: July 20, 2006)

The ferroelectricity of single-domain ultrathin $PbTiO_3$ films sandwiched between metallic Pt electrodes has been studied using *ab initio* density-functional theory (DFT) calculations within the local-density approximation. For stress-free $PbTiO_3$ films with an in-plane lattice constant of the tetragonal bulk phase we find that the films lose ferroelectricity below a critical thickness of about 4 and 6 unit cells ($\sim$16 Å and 24 Å) for PbO– and TiO_2–terminated films, respectively. This result is in contradiction to a recent DFT study by Sai, Kolpak and Rappe [Phys. Rev. B **72**, R020101 (2005)], in which the persistence of ferroelectricity for Pt/$PbTiO_3$/Pt films down to one unit cell (4 Å) has been reported. Careful tests with different types of pseudopotentials and density-functionals reveal that this discrepancy is due to insufficiencies of the widely used generalized-gradient approximations PW91 and PBE, which have been employed by Sai *et al.* for describing perovskite compounds.

PACS numbers: 77.80.-e, 77.84.Dy, 77.22.Ej, 31.15.Ar

Ultrathin ferroelectric (FE) perovskite films, epitaxially grown on perovskite substrates, have attracted considerable attention in the past years owing to their prospective application for non-volatile FE random access memory (FERAM) devices. Much effort has been contributed both in experiment and theory to study the FE properties of such ultrathin films[1]. An issue of particular importance is the question how thin perovskite films can be made before the ferroelectricity vanishes due to intrinsic finite size effects. Based on early experiments[2] it was assumed that ferroelectricity in thin films becomes suppressed below a critical thickness of about 10 nm. More recent studies showed, however, that stable FE phases exist for films as thin as a few nanometers[3–5]. Theoretical investigations even suggested that a FE polarization perpendicular to the surface can exist in films with a thickness of m=3 unit cells ($\sim$12 Å), if the depolarization field is removed by ideal electrodes[6,7]. Real metallic electrodes, however, have only a limited screening capability, and it has to be investigated if real electrodes are able to suppress the depolarization field well enough that ultrathin films are indeed in a FE state. For a chosen combination of electrode metal and perovskite material, the FE properties will be furthermore affected by the specific atomic relaxations, chemical interactions, and elastic stresses at the metal–oxide interface.

A first study to elucidate the existence of a minimum thickness for ferroelectricity in ultrathin perovskite films between realistic electrodes was carried out by Junquera and Ghosez[8]. Using *ab initio* density-functional theory (DFT) calculations within the local-density approximation (LDA) they found that ultrathin single-domain $BaTiO_3$ films in a capacitor geometry between conducting $SrRuO_3$ electrodes, epitaxially grown on a $SrTiO_3$ substrate which determines the lateral lattice parameter, lose their ferroelectricity below a thickness of about m=6 unit cells ($\sim$24 Å), thus suggesting that indeed a critical thickness exists for realistic FE films. In a more recent communication, however, Sai, Kolpak and Rappe[9] reported that ultrathin $PbTiO_3$ films between Pt and $SrRuO_3$ electrodes maintain their FE polarization normal to the interfaces even for film thicknesses of m=1 and m=2 unit cells (less than 10 Å), concluding that the behavior of $BaTiO_3$ is not universal for all FE thin films. In contrast to Junquera and Ghosez[8], Sai *et al.*[9] used the generalized gradient approximation (GGA) in their DFT study, and the in-plane lattice parameter of the thin films was set to the *experimental* lattice constant of the tetragonal bulk phase of $PbTiO_3$.

In previous investigations it was shown[10,11] that the commonly used GGA functionals such as PW91[12] and PBE[13] give rather poor results for the equilibrium structural parameters of bulk $PbTiO_3$ in the tetragonal phase. The c/a–ratio and the FE displacements of the atoms are much overestimated compared to experimental results. In the present paper we demonstrate that this poor performance of the PW91 and PBE functionals for the $PbTiO_3$ bulk phase furthermore leads to a substantial overestimation of the ferroelectricity in ultrathin $PbTiO_3$ films. Instead, traditional LDA[14,15] calculations tend to give more reliable results. An estimate of the critical thickness for ferroelectricity in single-domain Pt/$PbTiO_3$/Pt films appearing in a LDA setup will be given. This critical thickness depends strongly on the in-plane lattice parameter a, imposed by epitaxial growth of the films on a substrate[16,17], and the dependence of the ferroelectricity of the $PbTiO_3$ films on this parameter will be illustrated.

In our *ab initio* DFT calculations we used a very similar setup as Sai *et al.*[9] in their study. The computations were performed using the mixed-basis pseudopotential (MBPP) code[18] employing norm-conserving pseudopotentials[19] and a mixed basis set[20–23] of plane waves (with a cutoff energy of 20 Ry = 272 eV) and localized basis functions (for more details see Ref. 24). The pseudopotential approximation was carefully tested

TABLE I: Calculated equilibrium structural parameters of cubic and tetragonal bulk $PbTiO_3$ employing different computational methodologies and density-functionals. The optimized lattice parameter a (in Å), the tetragonal distortion c/a of the unit cell, and the internal coordinates u_z (in fraction of the lattice constant c) of the Ti, O_1 and O_3 atom are listed. The position of the Pb atom is fixed to u_z(Pb)=0. E_{gap} is the band gap in eV, and ΔE is the energy difference between tetragonal FE and cubic PE phase in eV per unit cell.

	cubic phase		tetragonal phase						
	a	E_{gap}	a	c/a	u_z(Ti)	$u_z(O_1)$	$u_z(O_3)$	E_{gap}	ΔE
LDA, MBPP	3.880	1.55	3.853	1.050	0.5312	0.0923	0.6012	1.62	−0.053
LDA, PAW	3.894	1.48	3.867	1.043	0.5334	0.0883	0.6018		−0.056
LDA[10]	3.894		3.858	1.051					
PW91, MBPP	3.957	1.69	3.827	1.247	0.5571	0.1938	0.6670	2.04	−0.196
PW91, PAW	3.969	1.61	3.841	1.233	0.5559	0.1859	0.6660		−0.192
PBE, MBPP	3.962	1.69	3.836	1.244	0.5579	0.1949	0.6675	2.05	−0.208
PBE[10]	3.971		3.857	1.230					
Exp.(298 K)[32,33]	3.969		3.905	1.064	0.539	0.114	0.617	3.5	

by repeating sets of calculations employing ultrasoft pseudopotentials (USPP)[25] and the projector augmented wave (PAW) method[26] as implemented in the Vienna Ab Initio Simulation Package VASP[27,28]. The USPP and PAW projectors provided by the VASP package were used together with a plane-wave cutoff energy of 500 eV. The Brillouin-zone integrations were carried out with 6×6×6 and 6×6×1 Monkhorst-Pack[29] k-point meshes together with a 0.2 eV Gaussian broadening[30] for the calculations of bulk and thin-film $PbTiO_3$, respectively.

The ultrathin (001)-oriented $PbTiO_3$ films between Pt electrodes were represented by electrode-perovskite-electrode multilayer models of the form Pt_3/TiO_2-(PbO-$TiO_2)_m/Pt_3$ and Pt_3/PbO-(TiO_2-PbO$)_m/Pt_3$ for the two possible (001)-surface terminations of the perovskite structure, where m is the number of perovskite unit cells in the $PbTiO_3$ film (the same notation as in Ref. 9 is used, see Fig. 1 therein). Instead of the electrode/perovskite superlattice geometry as in Ref. 9, which requires a strain relaxation along the surface normal direction, we included a vacuum region in our supercell models to separate the three Pt–layer thick top and bottom metal electrodes of the perovskite films. It was demonstrated recently by Kolpak *et al.*[31] that both supercell models give equivalent electrical short-circuit conditions.

The cubic paraelectric (PE) state of bulk $PbTiO_3$ and the thin films was obtained by a full atomic relaxation of the corresponding supercells with imposed centrosymmetry. To determine the FE state, a soft-mode distortion of the atoms was superimposed to the PE configuration, similar as in Ref.[8], followed by a full relaxation of all atomic positions normal to the interfaces. The configurations were considered as relaxed when the maximum force on the atoms was less than 0.01 eV/Å.

A very important issue is the proper choice of the in-plane lattice constant a to be used for the thin film geometries. An artificial compression of the in-plane lattice constant will cause an increase of the c/a–ratio, which in turn will enhance the preference of the FE state. Experimentally, $SrTiO_3$ and the tetragonal phase of $PbTiO_3$ have almost the same lattice constant of a=3.905 Å. This is why $SrTiO_3$ is often used as a substrate to grow stress-free FE $PbTiO_3$ films. In the LDA, the equilibrium lattice constant for $SrTiO_3$ is found[24] to be a=3.845 Å, which is very close to the LDA result for tetragonal $PbTiO_3$ (see Table I). Therefore we think that a=3.845 Å is the appropriate in-plane lattice constant in LDA calculations to simulate stress-free $PbTiO_3$ thin films. However, neither for a=3.845 Å nor for a=3.905 Å we found a FE state in our LDA calculations for m=2 thin films as reported by Sai *et al.*[9]. To make sure that we do not miss the FE configuration in our structural relaxation we applied the following procedure: we reduced the lattice parameter a until a FE configuration was obtained. Then we increased a step-by-step and re-relaxed all atoms until the FE state became higher in energy than the PE state.

In Table I we show the equilibrium structural parameters of bulk $PbTiO_3$ in the cubic and tetragonal phase as calculated with our different methodologies using LDA and GGA functionals. No significant differences between the two methodologies (i.e. PAW vs. MBPP) were found. The excellent agreement with previously published values[10] (as well as with the results from Refs. 11 and 34 which are not included in the table) confirms the validity of our calculations. The lattice parameter a is fairly well reproduced by both LDA and GGA within 1% deviation from the experimental value. In contrast, the tetragonal distortion c/a obtained by the GGA functionals is considerably larger, while the LDA result agrees very well with experiment. The FE displacements of the atoms again are much larger in the GGA than in the LDA, as is the energy difference ΔE between the tetragonal FE and cubic PE state. Overall, these results demonstrate that LDA clearly gives more realistic results for the structural parameters of tetragonal bulk phase of $PbTiO_3$ compared to experiment, whereas the GGAs substantially overestimate the FE distortions and favor by a great amount the stability of the FE state (with almost a factor 4 for the energy difference between the FE and PE state).

It is typical for DFT calculations to underestimate band gaps with respect to experiment (see Table I). The

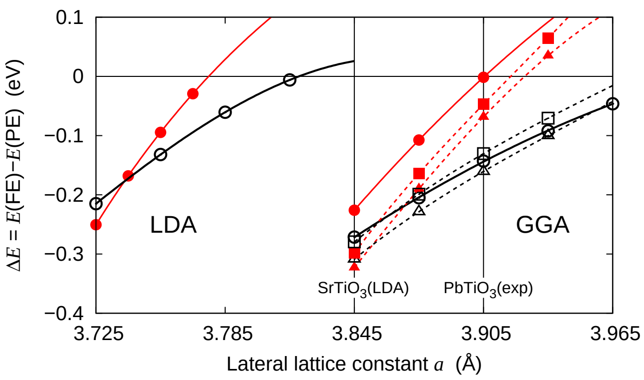

FIG. 1: (color online) Energy difference ΔE per perovskite unit cell between the FE and PE state for $PbTiO_3$ films with a thickness of m=2 as a function of the in-plane lattice parameter a. Filled and open symbols are for TiO_2– and PbO–terminated films, respectively (solid lines: MBPP, dashed with squares: USPP, dashed with triangles: PAW). The curves on the right are PW91, the two curves on the left are LDA calculations.

(a) PbO–terminated

(b) TiO_2–terminated

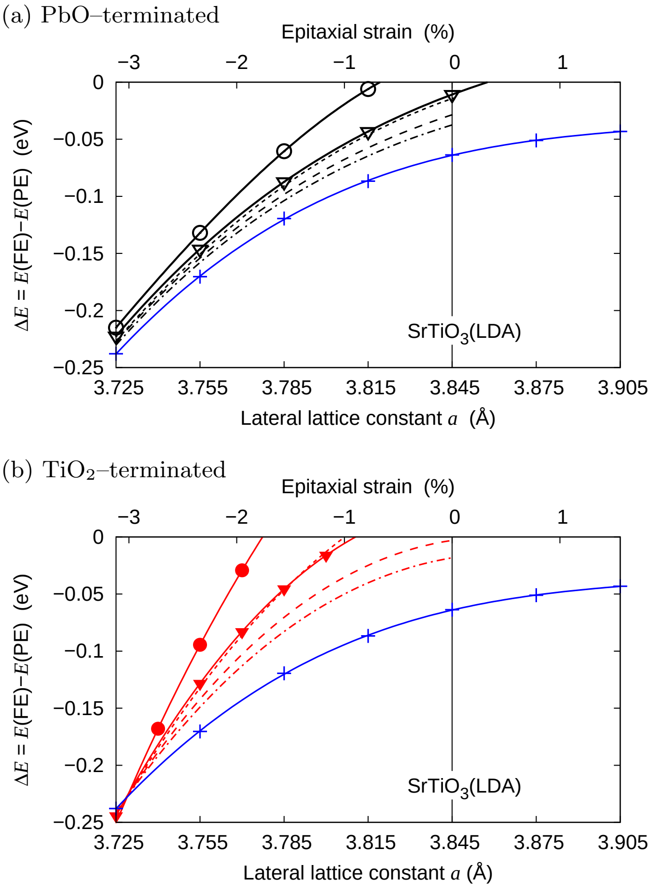

FIG. 2: (color online) Ferroelectric stability ΔE per perovskite unit cell of $PbTiO_3$ layers for different film thicknesses m as a function of the in-plane lattice constant a. The solid lines are fits to DFT–LDA data (circles: m=2, triangles: m=4, pluses: $m=\infty$). The short dashed, long dashed and dotted-dashed lines are extrapolated data for m=4, m=6 and m=8, respectively (see text).

minor improvement of the band gaps in GGA compared to LDA is mainly due to the larger equilibrium volume. To make sure that the underestimated band gaps do not lead to unphysical artefacts for the Pt/$PbTiO_3$ interfaces due to a positioning of the Fermi energy into the conduction band, i.e. a negative Schottky barrier for electrons, we have analyzed the alignment of the valence and conduction band edges of $PbTiO_3$ with respect to the Fermi level by inspecting the local density of states at an O atom in the central layer of the $PbTiO_3$ films. For the cubic Pt/$PbTiO_3$/Pt films and an in-plane lattice constant of a=3.845 Å we find within the MBPP–LDA setup that the valance band edge is 0.66 eV and 1.31 eV below and the conduction band edge is 0.76 eV and 0.33 eV above the Fermi energy for the PbO– and the TiO_2–terminated films, respectively. These values change slightly with the in-plane lattice constant a, but the Fermi energy remains located well inside the $PbTiO_3$ band gap.

Since in a thin film geometry the c/a–ratio and the FE distortions normal to the surfaces are not constrained and are allowed to relax freely, we can expect that the GGAs will artificially overestimate the preference of ferroelectricity in ultrathin layers. Even in the presence of a residual depolarization field due to incomplete screening by the electrodes, the strong energy gain in the GGA can be sufficient to stabilize the FE state, whereas in the LDA the FE state remains suppressed. Such a behavior is clearly present in Fig. 1, where we plotted the energy difference per perovskite unit cell ΔE between the FE and PE state for the m=2 thin films as a function of the in-plane lattice parameter a. Again, our different methodologies, MBPP, PAW and USPP, give very consistent results. As expected, ΔE strongly increases as a function of a, until it finally becomes positive. A pronounced difference in the stability of the FE state depending on the chemical nature of the metal–oxide interface is found. For the PbO–terminated films ferroelectricity is supported up to a larger lattice constant a than for the TiO_2–terminated layers.

Our GGA results are in excellent agreement with data from Sai *et al.*[9], who obtained an energy difference of ΔE=−0.05 eV and ΔE=−0.19 eV for the TiO_2– and PbO–terminated m=2 films at the experimental lattice constant a=3.905 Å of tetragonal bulk $PbTiO_3$[35]. However, the GGAs and LDA give significantly different quantitative results for the stability of the FE states of the films. The GGAs predict a FE ground state even for lattice parameters above the theoretical and experimental values of a, whereas in LDA a strong lateral compression of the films would be required to obtain a stable FE state. In view of our results for the FE structure and stability of the $PbTiO_3$ bulk phase as shown in Table I, the LDA results can be considered to be much more reliable than the GGA calculations. The substantial overestimation of ferroelectricity in $PbTiO_3$ seems to be a general property of the PW91– and PBE–GGA functionals[10,11]. However, Wu and Cohen[11] recently proposed a modification of the PBE functional, which leads to a greatly improved description of ferroelectricity in bulk $PbTiO_3$ and which promises to be more accurate than the LDA.

Finally, we determined the critical thickness of the $PbTiO_3$ films which is required within the LDA to stabilize a FE ground state. Figure 2 shows the result for ΔE per perovskite unit cell versus a for different film thicknesses m as calculated with the MBPP method. Additionally, the limit for $m{=}\infty$ is plotted, which is obtained from bulk calculations imposing the respective value of a. At the theoretical equilibrium lattice constant of $SrTiO_3$ of a=3.845 Å we find that the m=4 PbO–terminated films have become ferroelectric. The m=4 TiO_2–terminated films stay paraelectric unless the lattice parameter is compressed to be below 3.815 Å. Using the extrapolation formula

$$\Delta E_{\mathrm{est}}(m{=}4) = \Big(2\Delta E(m{=}2) + 2\Delta E(m{=}\infty)\Big)/4 \quad (1)$$

we calculated an estimate of ΔE for the m=4 geometry. The result, plotted by short-dashed lines in Fig. 2, is almost identical to the full m=4 DFT calculations. This indicates that only the outermost unit cell of the perovskite layer is significantly affected by the metal layer, whereas the inner unit cells already possess the bulk-like properties. Hence, we can refrain from doing full DFT calculations for increased film thicknesses and use the extrapolation scheme instead. Extrapolating correspondingly the ΔE results for m=4 to m=6 and m=8 we find that at a=3.845 Å ΔE has become negative for both surface terminations, indicating that the critical thickness of the TiO_2–terminated film is around m=6 or 24 Å.

In summary, we have investigated the stability of the FE state of ultrathin Pt/$PbTiO_3$/Pt films based on *ab initio* DFT–LDA calculations. We find that the films posses a critical thickness below which the FE state becomes unstable, which we estimated to be about 16 Å and 24 Å for PbO– and TiO_2–terminated films, respectively. However, using the GGA functionals PW91 and PBE we get significantly different results. The films stay ferroelectric down to a thickness below two unit cells as also recently reported by Sai *et al.*[9] Since PW91 and PBE have severe deficiency to describe correctly the bulk FE state of $PbTiO_3$, this prediction of a much smaller critical thickness is not stringent.

We acknowledge financial support for YU from the Grant-in-Aid for Scientific Research of the Japan Society of the Promotion of Science (JSPS) and the Center of Excellence for Research and Education on Complex Functional Mechanical Systems (COE program of the Ministry of Education, Culture, Sports, Science and Technology, Japan), for CE from the German Research Foundation (project EL 155/17-1 in the DFG priority program SPP 1157 "Integrated electroceramic functional structures"), and for PG from the European Commission (contract Nr. NMP3-CT-2005-013862 (INCEMS)).

[1] M. Dawber, K.M. Rabe, and J.F. Scott, Rev. Mod. Phys. **77**, 1083 (2005).
[2] T. Maruyama, M. Saitoh, I. Sakai, T. Hidaka, Y. Yano, and T. Noguchi, Appl. Phys. Lett. **73**, 3524 (1998), and references therein.
[3] T. Tybell, C.H. Ahn, and J.M. Triscone, Appl. Phys. Lett. **75**, 856 (1999).
[4] N.A. Spaldin, Science **304**, 1606 (2004); D.D. Fong, G.B. Stephenson, S.K. Streiffer, J.A. Eastman, O. Auciello, P.H. Fuoss, and C. Thompson, Science **304**, 1650 (2004).
[5] C. Lichtensteiger, J.M. Triscone, J. Junquera, and P. Ghosez, Phys. Rev. Lett. **94**, 047603 (2005).
[6] P. Ghosez, K.M. Rabe, Appl. Phys. Lett. **76**, 2767 (2000).
[7] B. Meyer, D. Vanderbilt, Phys. Rev. B **63**, 205426 (2001).
[8] J. Junquera and P. Ghosez, Nature **422**, 506 (2003).
[9] N. Sai, A.M. Kolpak, and A.M. Rappe, Phys. Rev. B **72**, 020101(R) (2005).
[10] Z. Wu, R.E. Cohen, and D.J. Singh, Phys. Rev. B **70**, 104112 (2004).
[11] Z. Wu and R.E. Cohen, Phys. Rev. B **73**, 235116 (2006).
[12] J.P. Perdew, J.A. Chevary, S.H. Vosko, K.A. Jackson, M.R. Pederson, D.J. Singh, and C. Fiolhais, Phys. Rev. B **46**, 6671 (1992); (E): Phys. Rev. B **48**, 4978 (1993).
[13] J.P. Perdew, K. Burke, and M. Ernzerhof, Phys. Rev. Lett. **77**, 3865 (1996); (E): Phys. Rev. Lett. **78**, 1396 (1997).
[14] D. Ceperley and B. Alder, Phys. Rev. Lett. **45**, 566 (1980).
[15] J.P. Perdew and A. Zunger, Phys. Rev. B **23**, 5048 (1980).
[16] O. Diéguez, K.M. Rabe, and D. Vanderbilt, Phys. Rev. B **72**, 144101 (2005).
[17] C. Ederer and N.A. Spaldin, Phys. Rev. Lett. **95**, 257601 (2005).
[18] B. Meyer, F. Lechermann, C. Elsässer, and M. Fähnle, Fortran90 Program for Mixed-Basis Pseudopotential Calculations for Crystals, Max-Planck-Institut für Metallforschung, Stuttgart.
[19] D. Vanderbilt, Phys. Rev. B **32**, 8412 (1985).
[20] C. Elsässer, N. Takeuchi, K.M. Ho, C.T. Chan, P. Braun, and M. Fähnle, J. Phys.: Condens. Matter **2**, 4371 (1990).
[21] K.M. Ho, C. Elsässer, C.T. Chan, and M. Fähnle, J. Phys.: Condens. Matter **4**, 5189 (1992).
[22] B. Meyer, K. Hummler, C. Elsässer, and M. Fähnle, J. Phys.: Condens. Matter **7**, 9201 (1995).
[23] F. Lechermann, F. Welsch, C. Ederer, C. Elsässer, M. Fähnle, J.M. Sanchez, and B. Meyer, Phys. Rev. B **65**, 132104 (2002).
[24] T. Ochs and C. Elsässer, Z. Metallkd. **93**, 406 (2002).
[25] D. Vanderbilt, Phys. Rev. B **41**, 7892 (1990).
[26] P. Blöchl, Phys. Rev. B **50**, 17953 (1994).
[27] G. Kresse and J. Hafner, Phys. Rev. B **47**, 558 (1993).
[28] G. Kresse, J. Furthmüller, Phys. Rev. B **54**, 11169 (1996).
[29] H.J. Monkhorst, J.D. Pack, Phys. Rev. B **13**, 5188 (1976).
[30] C.L. Fu and K.M. Ho, Phys. Rev. B **28**, 5480 (1983).
[31] A.M. Kolpak, N. Sai, and A.M. Rappe, cond-mat/0512670.
[32] A.M. Glazer and S.A. Mabud, Acta Cryst. **34**, 1065 (1978).
[33] J. Robertson and C.W. Chen, Appl. Phys. Lett. **74**, 1168 (1999).
[34] B. Meyer, J. Padilla, and D. Vanderbilt, Faraday Discuss. **114**, 395 (1999).
[35] Unpublished data provided by the authors of Ref. 9.